Ursolic acid protects against cisplatin-induced ototoxicity by inhibiting oxidative stress and TRPV1-mediated Ca^{2+}-signaling

YANG DI[1*], TAO XU[2*], YUAN TIAN[1], TINGTING MA[1], DONGHAO QU[1], YAN WANG[1], YUHAN LIN[1], DONGYAN BAO[1], LI YU[1], SHUANGYUE LIU[1] and AIMEI WANG[1]

[1]Department of Physiology and [2]Life Science Institute, Jinzhou Medical University, Jinzhou, Liaoning 121000, P.R. China

Received October 20, 2019; Accepted May 13, 2020

DOI: 10.3892/ijmm.2020.4633

Abstract. Cisplatin (CDDP) is widely used in clinical settings for the treatment of various cancers. However, ototoxicity is a major side effect of CDDP, and there is an associated risk of irreversible hearing loss. We previously demonstrated that CDDP could induce ototoxicity via activation of the transient receptor potential vanilloid receptor 1 (TRPV1) pathway and subsequent induction of oxidative stress. The present study investigated whether ursolic acid (UA) treatment could protect against CDDP-induced ototoxicity. UA is a triterpenoid with strong antioxidant activity widely used in China for the treatment of liver diseases. This traditional Chinese medicine is mainly isolated from bearberry, a Chinese herb. The present results showed that CDDP increased auditory brainstem response threshold shifts in frequencies associated with observed damage to the outer hair cells. Moreover, CDDP increased the expression of TRPV1, calpain 2 and caspase-3 in the cochlea, and the levels of Ca^{2+} and 4-hydroxynonenal. UA co-treatment significantly attenuated CDDP-induced hearing loss and inhibited TRPV1 pathway activation. In addition, UA enhanced CDDP-induced growth inhibition in the human ovarian cancer cell line SKOV3, suggesting that UA synergizes with CDDP *in vitro*. Collectively, the present data suggested that UA could effectively attenuate CDDP-induced hearing loss by inhibiting the TRPV1/Ca^{2+}/calpain-oxidative stress pathway without impairing the antitumor effects of CDDP.

Correspondence to: Professor Shuangyue Liu or Professor Aimei Wang, Department of Physiology, Jinzhou Medical University, 40, Section 3, Songpo Road, Linghe, Jinzhou, Liaoning 121000, P.R. China
E-mail: liushuangyue@jzmu.edu.cn
E-mail: wangaimei@jzmu.edu.cn

*Contributed equally

Key words: ursolic acid, cisplatin, cochlea, calcium ion, transient receptor potential vanilloid receptor 1, calpain, 4-hydroxynonenal

Introduction

Cisplatin (CDDP) is a divalent platinum compound with broad-spectrum anticancer activity that synergizes with a variety of antitumor drugs without cross-resistance, making it a first-line anticancer drug (1). CDDP is commonly used for the treatment of various cancers including bladder cancer, lung cancer, ovarian cancer and other soft tissue tumors. In children, CDDP is also effective for the treatment of various solid tumors (2,3). However, CDDP has serious side effects, including irreversible hearing loss, especially in juvenile patients treated with CDDP and radiotherapy for at least six months (4-6).

The mechanism of CDDP-induced ototoxicity remains to be elucidated. CDDP could induce apoptosis of cochlear cells, which led to hearing loss (7-9). Several studies also showed that CDDP increased NADPH oxidase 3 (NOX 3) expression in the cochlea, which increased the production of reactive oxygen species (ROS) (10,11). ROS directly attacked the cochlear cell membrane and produced the toxic lipid peroxidation product 4-hydroxynonenal (4-HNE), which might also account for cochlear cell apoptosis (12). A study showed that CDDP-induced ototoxicity in the cochlea was related to calcium (Ca^{2+}) overload (13). As an important second messenger, Ca^{2+} is involved in various functions, including auditory signal transduction (14). Moreover, maintenance of a low intracellular Ca^{2+} concentration in the normal resting state plays an important role in sustaining homeostasis (15). Abnormal influx of free Ca^{2+} in cells (referred to as Ca^{2+} overload) can cause structural damage and disruption of intracellular metabolism of hair cells (HCs), eventually leading to apoptosis of HCs (16). In the cochlea, Ca^{2+} overload was related to high expression of the transient receptor potential vanilloid receptor 1 (TRPV1) (17). TRP channels are a family of non-selective cation ion channels that control important cellular functions and signaling pathways (18). TRP channels are also important targets for a wide range of drugs, such as menthol, which adjust human TRP melastatin 8 (hTRPM8)-induced signaling, and could alleviate hyperglycemia in alloxan-treated mice (a model of type 1 diabetes) or reverse muscle atrophy in dexamethasone-treated mice (a model of muscle wasting) (19). TRP channel activation can lead to changes in Ca^{2+} homeostasis, resulting in long lasting modulation of Ca^{2+} levels (20,21). TRPV1 is expressed in many organs, including the heart, kidney, brain, dorsal root ganglions and sensory neurons (22). TRPV1 plays a critical role in the maintenance of cellular homeostasis, particularly

in cochlear cells (23). Studies have suggested that CDDP induced Ca^{2+} overload by increasing TRPV1 expression, and that Ca^{2+} subsequently activates calpain, a neutral cysteine protease, to cause cochlear apoptosis (24). However, the association between Ca^{2+} overload and TRPV1 remains to be confirmed.

Ursolic acid (UA) is a plant-derived triterpene compound with strong antioxidant effects (25-27). UA is the main ingredient of several traditional Chinese herbal medicines used in the treatment of liver diseases and in lowering blood lipid (28,29). In PC12 cells, UA could assert its neuroprotective effects by inhibiting ROS production induced by amyloid beta peptide (30,31). In addition, UA could capture oxygen free radicals in the P450 monoamine oxidase system and liver microsome, thus exerting a strong inhibitory effect on lipid peroxidation (32). However, to the best of our knowledge, there are currently no reports on the anti-apoptotic and anti-oxidative effects of UA on ototoxicity induced by CDDP. The present study evaluated the protective effects of UA on CDDP-induced ototoxicity and the underlying mechanisms were investigated. It was hypothesized that UA could protect against CDDP-induced ototoxicity by inhibiting oxidative stress and TRPV1-mediated Ca^{2+}-signaling in the cochlear cells.

Materials and methods

Animal and experimental protocols. A total of 48 BALB/c mice (3 days) were purchased from the Animal Experimental Center, Jinzhou Medical University, China. A total of 48 BALB/c mice (20-22 g, 4 weeks, male and female) with normal Preyer's reflexes were purchased from the Animal Experimental Center, Dalian Medical University, China [license no. SCXK (Liao) 2008-0002]. All animal studies complied with the regulations for the Management of Laboratory Animals published by the Ministry of Science and Technology of the People's Republic of China, and all animal protocols were approved by the Animal Care and Use Committee of Jinzhou Medical University. All mice were fed a standard commercial diet and housed at an ambient temperature of 20-24˚C with a relative humidity of 50±5% under a 12/12 h light-dark cycle in a specific pathogen-free facility during the experiment. All animals were allowed 1 week to acclimate before treatment and then were randomly divided into four groups (n=12 in each group) and treated for five days as follows: i) Normal control group, where the mice received physiological saline [0.5 ml/100 g, intraperitoneally (i.p)]; ii) UA group, where the mice received UA (purity ≥98%; cat. no. N1823, APExBIO Technology LLC; 80 mg/kg/day, i.p); iii) CDDP group, where the mice received CDDP (Sigma-Aldrich; Merck KGaA; 4.5 mg/kg/day, i.p,) and iv) UA plus CDDP (UA+CDDP) group, where the mice received UA (80 mg/kg/day, i.p) followed by CDDP (4.5 mg/kg/day, i.p) 30 min later each day (Fig. 1A).

During the treatment period, the weight of the experimental animals was measured every day (Fig. S1). Although CDDP is toxic, the survival rate of mice is 100% during the administration (33).

Measurement of auditory brainstem response (ABR). For the analysis of the auditory threshold, ABR was recorded 1 day before and 5 days after related drug treatment with tone bursts of 8, 12 and 24 kHz using the Smart EP & OAE auditory evoked potential recording system (Intelligent Hearing Systems). The mice were anesthetized using pentobarbital sodium (90 mg/kg) and kept warm with a heating pad during ABR recording. A subdermal (active) needle electrode was inserted at the vertex, while ground and reference electrodes were inserted subdermally in the loose skin beneath the pinnae of opposite ears. The technique used to record ABRs has been previously described in detail (34). The ABR waveforms were averaged over a 10 msec time window using the Smart EP & OAE auditory evoked potential recording system software (Launch Pad 2.32 HIS program). The sound intensity was varied at 5 dB intervals near the hearing threshold. The differences in ABR thresholds shift for each frequency between the starting and the terminal points of the experimental time course were noted. The threshold was determined off-line by two independent, experimentally blinded observers based on the ABR records. In addition, the mice were euthanized, and double cochleae were removed for further analysis.

Outer hair cell (OHC) counting. Immediately after completion of the ABR test, the animals were killed by cervical dislocation under anesthesia with an intraperitoneal injection of pentobarbital sodium (90 mg/kg). An array of criteria was used to verify the death of animals, including absence of respiration and heartbeat and loss of corneal and palpebral reflexes.

The temporal bones were removed, and the cochlea was immersed in 4% paraformaldehyde and incubated overnight at 4˚C. The cochlea was decalcified in 4% EDTA for 7 days at 4˚C. Subsequently, the basilar membrane was dissected under a dissecting microscope, and the stria vascularis and tectorial membrane were removed. The basilar membrane was then stained with phalloidin-tetramethylrhodamine (TRITC; Sigma-Aldrich; Merck KGaA) for 20 min at 20-24˚C and protected from light. The specimens were then rinsed three times with 0.01 M phosphate-buffered saline (PBS; pH 7.4) and then mounted on slides. Images were obtained using the TCS-SP5 II laser-scanning confocal microscope (Leica Biosystems GmbH). Outer hair cells were counted from the captured images using a fluorescent BX41 microscope (Olympus Corporation) at x200 magnification in 20 consecutive fields from the apex to the basal turn along the entire length of the cochlear epithelium. The percentages of outer hair cell loss in each 0.5-mm length of epithelium were plotted as a function of the cochlear length as a cytocochleogram (34).

Immunohistochemical staining of paraffin sections of the cochlea. After the last auditory brainstem response test, five mice from each group were decapitated under abdominal anesthesia using pentobarbital sodium (90 mg/kg), and the temporal bones were removed immediately. The round and oval windows were opened, cochleae were perfused with 40 g/l paraformaldehyde (pH 7.4), and the specimens were immersed in the 4% paraformaldehyde for 24 h at 4˚C. Following decalcification in 40 g/l EDTA solution (pH 7.4) for 5 days at 4˚C, the cochleae were dehydrated with ethanol, cleared with xylene and embedded in paraffin wax. Serial sections (5-μm thickness) were prepared, dewaxed, rehydrated

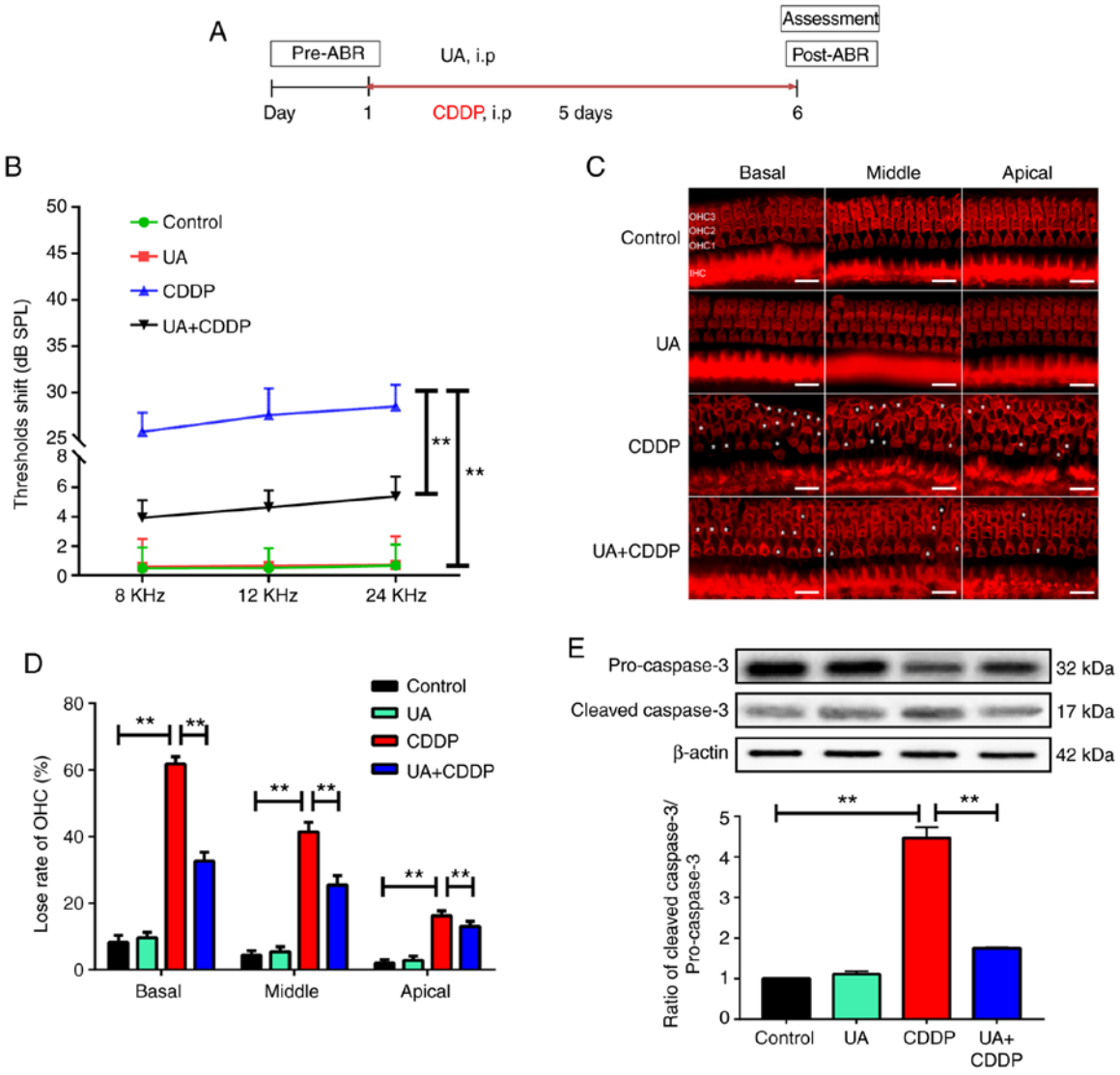

Figure 1. UA prevents CDDP-induced hearing loss and cochlea apoptosis in mice. (A) The flow chart of the experimental protocol. (B) ABR results at tone bursts of 8, 12, 24 kHz. n=12 mice for each group. **P<0.01. (C) UA prevented CDDP-induced OHC loss. OHCs were labeled by tetramethylrhodamine-phalloidin staining in the basilar membrane. White asterisks indicate cell loss. Scale bar, 20 μm. OHCs exhibited regional variation in their susceptibility to cisplatin, with gradual severity of hair cell loss from the apical turn to the basal turn. Mice receiving UA + CDDP demonstrated fewer OHC loss. (D) The numbers of intact hair cells on the apical, middle and basal turns. The graph shows quantitative differences of OHC loss at apical, middle and basal turns of the cochlear basilar membrane The UA + CDDP group exhibited significantly fewer hair cell loss in comparison compared with the CDDP group. n=3 ears for each group. **P<0.01 (E) Western blot analysis was performed to detect protein expression levels of cleaved caspase-3 and caspase-3 in cochlea, with β-actin as a loading control. n=6 ears for each group. Mean values were obtained from n=3 independent experiments. **P<0.01. ABR, auditory brainstem response; UA, ursolic acid; i.p, intraperitoneal; CDDP, cisplatin; OHC, outer hair cell; SPL, sound pressure levels.

in descending alcohol series, rinsed with distilled water and treated with high pressure (125˚C; 103 kPa; 3 min) to retrieve antigens. Endogenous peroxidase activity was blocked with 3 g/l H_2O_2 for 10 min at 20-24˚C, followed by a PBS wash. After incubation with normal goat serum (cat. no. C0265; Beyotime Institute of Biotechnology) for 15 min at 20-24˚C, tissue sections were stained overnight at 4˚C with primary antibodies for TRPV1 (1:500; cat. no. ab6166; Abcam) and calpain 2 (1:1,000; cat. no. sc-373967; Santa Cruz Biotechnology, Inc.). After washing with PBS, sections were stained with horseradish peroxidase-conjugated-biotinylated goat anti-rabbit immunoglobulin G (IgG) secondary antibody (1:1,000; cat. no. ab205718; Abcam) for 1 h at 20-24˚C. Following washing with PBS, color was developed with 0.05% 3,3'-diaminobenzidine for 3 min at 20-24˚C. Sections were counterstained with hematoxylin for 10 min at 20-24˚C, dehydrated with gradient concentrations of ethanol, vitrified with xylene and mounted with neutral gum. PBS was used as a negative control throughout the study. The sections were observed by using a BX41 fluorescent microscope at x400 magnification (Olympus Corporation). Relative optical intensity was determined using Image-Pro Plus 6.0 software (Media Cybernetics, Inc.).

Western blot analysis. Total cochlea tissue was homogenized in RIPA buffer (cat. no. P0013B; Beyotime Institute of Biotechnology) containing protease inhibitor cocktail tablets and phosphatase inhibitors cocktail (Roche Diagnostics GmbH). The tissue homogenate was sonicated for 30 sec and centrifuged at 14,000 x g at 4˚C for 30 min to extract the

supernatant. Protein concentrations were determined using a bicinchoninic acid kit. The protein samples (50 μg/lane) were separated using SDS-PAGE (7.5% for TRPV1 and calpain 2; 10% for 4-HNE and pro-caspase 3 and 12.5% for cleaved caspase 3). Following electrophoresis, the proteins were transferred onto nitrocellulose membranes (Thermo Fisher Scientific, Inc.). The membranes were then blocked with 10% bovine serum albumin for 1 h at 4˚C and incubated overnight at 4˚C with the following primary antibodies: Anti-TRPV1 (1:500; cat. no. ab6166; Abcam), anti-calpain 2 (1:1,000; cat. no. sc-373967; Santa Cruz Biotechnology, Inc.), anti-4-HNE (1:800; cat. no. ab48506; Abcam), anti-cleaved caspase-3 (1:1,000; cat. no. ab13847; Abcam) and anti-caspase-3 (1:1,000; cat. no. sc-7272; Santa Cruz Biotechnology, Inc.). After washing three times with TBS-0.05% Tween-20, membranes were incubated with IRDye 800CW goat anti-rabbit IgG secondary antibody (1:10,000; cat. no. 925-32211; LI-COR Biosciences.) for 1 h at 4˚C. Following extensive washing, the immunoreactive bands were visualized by ECL. The Odyssey CLx Infrared imaging system (LI-COR Biosciences) was used to analyze the optical density value of immunoreactive bands. β-actin (1:1,000; cat. no. sc-47778; Santa Cruz Biotechnology, Inc.) was used as a loading control.

Organotypic cultures of postnatal organ of Corti. The organ culture procedures were modified from a previously published report (35). In brief, Cochlear explants were isolated from newborn 3-day-old BALB/c mice. BALB/c pups were euthanized following antisepsis using 75% ethanol. The two otic capsules were extracted from surrounding tissue and immersed ice-cold Hank's balanced salt solution (HBSS; cat. nos. CC014 and CC016; M&C Gene Biotechnology). The lateral wall tissues (stria vascularis and spiral ligament) and the auditory nerve bundle were micro-dissected for sterile dissection under a binocular microscope (Olympus SZX7; Olympus Corporation). The explants were carefully placed onto a prepared culture dish containing a 15-μl polymerized drop of rat tail collagen in 1 ml culture medium consisting of DMEM/F12 (Invitrogen; Thermo Fisher Scientific, Inc.), 1% bovine serum albumin (Invitrogen; Thermo Fisher Scientific, Inc.), and 10 U/ml penicillin G. Following 4 h of incubation (37˚C, 5% CO_2), an additional 1 ml medium was added to submerge the explants.

Measurement of Ca^{2+} levels in OHCs. Cell-permeable Ca^{2+} indicator Fluo-4 AM (cat. no. F14201; Invitrogen; Thermo Fisher Scientific, Inc.) were used to monitor levels of intracellular Ca^{2+}, based on the literature (36). Following immersion in HBSS without Ca^{2+} and Mg^{2+} for 20 min at 20-24˚C, the organ explants were immersed in dye (cat. no. F14201; Invitrogen; Thermo Fisher Scientific, Inc.) for 25 min following Fluo4-AM loading at 24˚C. Subsequently, the explants were fixed in 4% paraformaldehyde for 30 min at 20-24˚C. Phalloidin (1:200) was applied for 1 h at 20-24˚C and protected from light. For measurement of Fluo-4 Ca^{2+} signals, organs were imaged under a BX41 microscope at x400 magnification (Olympus Corporation) with epifluorescence, and the images were obtained using a TCS-SP5II laser-scanning confocal microscope (x400 magnification; Leica Biosystems GmbH) in 20 consecutive fields.

Immunofluorescence for assessment of 4-HNE. Preparation of cochlear paraffin sections (5-μm thickness), deparaffinization, rehydration, antigen retrieval and blocking nonspecific binding were performed as described in a previous study (34). Tissue sections were incubated with rabbit anti-4-HNE antibody (1:200; cat. no. ab46545; Abcam), followed by Cy3-labeled goat anti-rabbit IgG secondary antibody (1:500; cat. no. A0516; Beyotime Institute of Biotechnology) incubation for 1 h at 24˚C. Immunofluorescence images were obtained via TCS-SP5II laser-scanning confocal microscopy (x400 magnification; Leica Biosystems GmbH). Relative optical intensity was determined using Image-Pro Plus 6.0 software (Media Cybernetics, Inc.).

Measurement of cell growth inhibition by MTT assay. The human ovarian cancer cell line SKOV3 (Peking Union Medical College, Beijing) were seeded at a density of $3x10^3$ cells/well in 96-well plates and treated with different concentrations (1, 2, 3, 4, 8, 10 and 16 μg/ml) of CDDP. Each concentration treatment was repeated in six separate wells. Cells treated with RPMI 1640 media (100 ul; Sigma-Aldrich; Merck KGaA) alone acted as a control. The cells were incubated at 37˚C with 5% CO_2 for 24 h, and MTT reagent (20 μl; 5 mg/ml in PBS; Sigma-Aldrich; Merck KGaA) was added to each well and incubated at 37˚C with 5% CO_2 for 4 h. The absorbance in each well was measured at a wavelength of 570 nm using an enzyme-linked immunoassay microplate reader. According to the tumor cell growth inhibition rate, 4 μg/ml of CDDP was determined as optimal inhibitory concentration. Subsequently, SKOV3 cells were seeded at a density of $3x10^3$ cells/well in a 96-well plate and treated with CDDP (4 μg/ml). Different concentrations (20, 40, 80 and 160 mol/l) of UA were added later. Each concentration of UA treatment was repeated in six separate wells. The cells were incubated at 37˚C with 5% CO_2 for 24 h, and MTT reagent (20 μl; 5 mg/ml in PBS; Sigma-Aldrich; Merck KGaA) was added to each well and incubated at 37˚C with 5% CO_2 for 4 h. The absorbance in each well was measured at a wavelength of 570 nm using an enzyme-linked immunoassay microplate reader (BioTek Instruments, Inc.).

Statistical analysis. Data are presented as the mean ± SD and were analyzed using SPSS 17.0 software (SPSS, Inc.). Intergroup differences in mean values were compared by one-way ANOVA followed by Tukey's post hoc test. $P<0.05$ was considered to indicate a statistically significant difference.

Results

UA prevents CDDP-induced hearing loss and hair cell loss in vivo. To investigate whether UA could prevent CDDP-induced hearing loss, the ABR test was performed on mice. In the control group, ABR thresholds at 8, 12, and 24 kHz were observed to be stable (0.48±1.43, 0.50±1.37 and 0.67±1.44 dB, respectively). However, ABR threshold shifts in the CDDP group were significantly increased at 8, 12 and 24 kHz (25.78±2.06, 27.59±2.86 and 28.51±2.32 dB, respectively), compared with the control group ($P<0.01$). In the UA + CDDP group, ABR threshold shifts significantly reduced at 8, 12 and 24 kHz ($P<0.01$; 3.93±1.19, 4.63±1.16

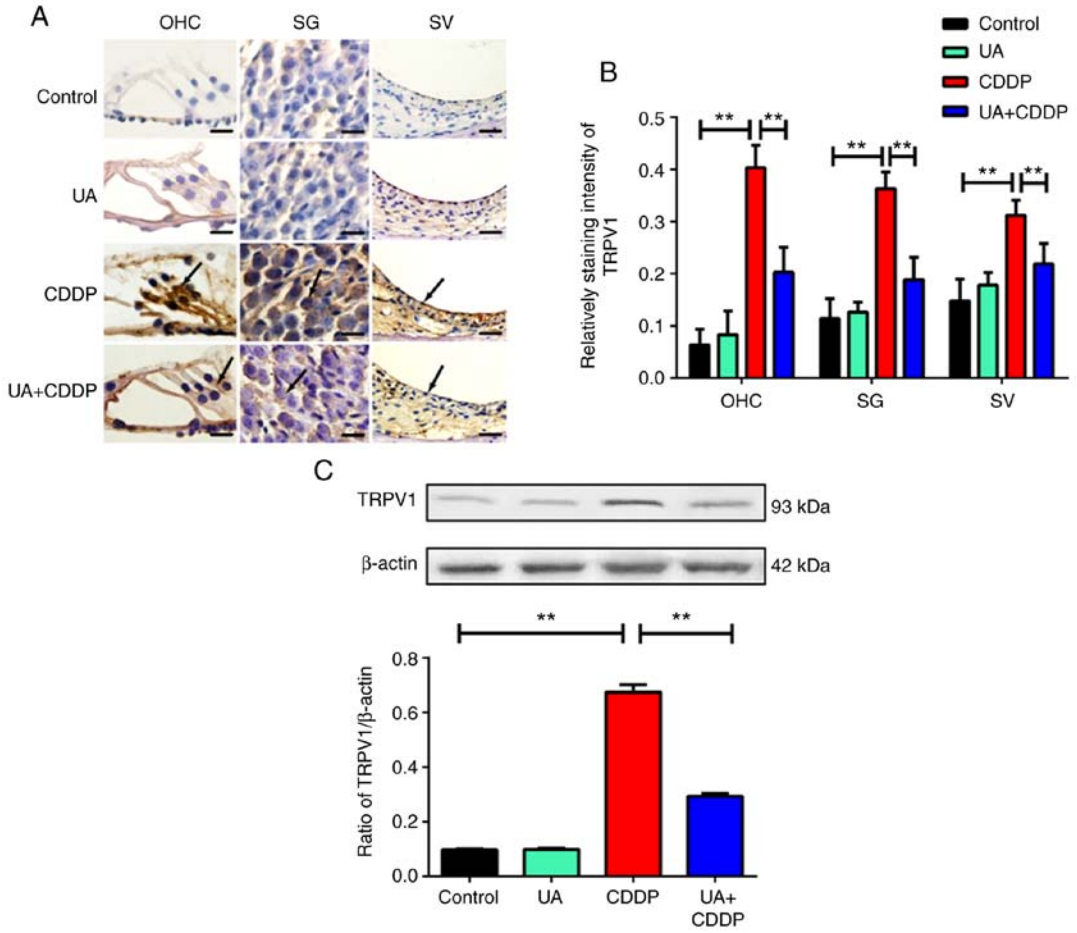

Figure 2. Effect of UA on CDDP-induced expression of TRPV1 in mouse cochlea. (A) Representative immunohistochemical staining images (brown and yellow granules) of TRPV1 on the organ of Corti, SG and SV of the cochleae. Arrows indicate the location of TRPV1-positive expression. Scale bar, 20 μm. (B) Quantification of TRPV1 immunolabeling in the different groups. n=3 ears for each group. **P<0.01. (C) Western blot analysis of TRPV1 was used to detect protein expression of TRPV1 in cochlea, with β-actin as a loading control. n=6 ears for each group. Mean values were obtained from n=3 independent experiments. **P<0.01. UA, ursolic acid; CDDP, cisplatin; SG, spiral ganglion; SV, stria vascularis; TRPV1, transient receptor potential vanilloid receptor 1.

and 5.38±1.36 dB, respectively), compared with the CDDP group. In the UA group, UA treatment alone did not affect the ABR threshold shifts compared with the control group. These results suggested that UA can mitigate CDDP-induced hearing loss in mice (Fig. 1B).

To further determine the *in vivo* protective effects of UA against CDDP, TRITC staining of OHCs was performed on the basilar membrane of mouse cochlea and the number of surviving OHCs was counted. In the control and UA groups, OHCs on the basilar membrane appeared normal in structure and the staining pattern was homogeneous. Moreover, the loss rate of OHCs at each turn of the basilar membrane was <10%. In the CDDP group, the stereocilia of OHCs were characterized by loss and disorder. OHCs exhibited regional variation in their susceptibility to cisplatin, with gradual severity of OHC loss from the apical to the basal turn, and loss rates of OHCs at apical, middle and basal turns reaching 16, 41 and 61%, respectively, which was significantly higher compared with the control group (P<0.01; Fig. 1C and D). However, compared with the CDDP group, animals receiving UA + CDDP demonstrated significantly fewer OHC loss, especially at basal and middle turns, with the loss rate of OHCs at apical, middle and basal turns reaching 13, 25 and 32%, respectively (P<0.01; Fig. 1C and D). These results suggested that UA effectively protects against CDDP-induced OHC structural damage. Numerous studies showed that CDDP mainly damaged OHCs, while the damage of inner hair cells was weak (8). Hence, the present study focused on the outer hair cell change in and inner hair cell counting was not investigated.

Western blot analysis showed that the CDDP group expressed significantly higher levels of cleaved caspase-3 protein (a marker for apoptosis) compared with the control group (P<0.01; Fig. 1E). By contrast, cleaved caspase-3 expression levels in the UA + CDDP group were significantly lower compared with the CDDP group (P<0.01; Fig. 1E). However, cleaved caspase-3 expression levels in the UA group were not significantly different compared with the control group (Fig. 1E). Again, these results are consistent with the notion that UA can prevent the auditory loss observed in mice treated with CDDP.

UA inhibits CDDP-induced activation of the TRPV1/Ca^{2+}/calpain 2 signaling pathway in the cochleae. Based on immunohistochemistry results (Figs. 2A and 3A), TRPV1 and calpain 2 were uniformly distributed on the OHCs, spiral ganglion (SG), and stria vascularis (SV) of the cochlea in the control group. By contrast, TRPV1 and calpain 2 staining was unevenly distributed in the CDDP group, and

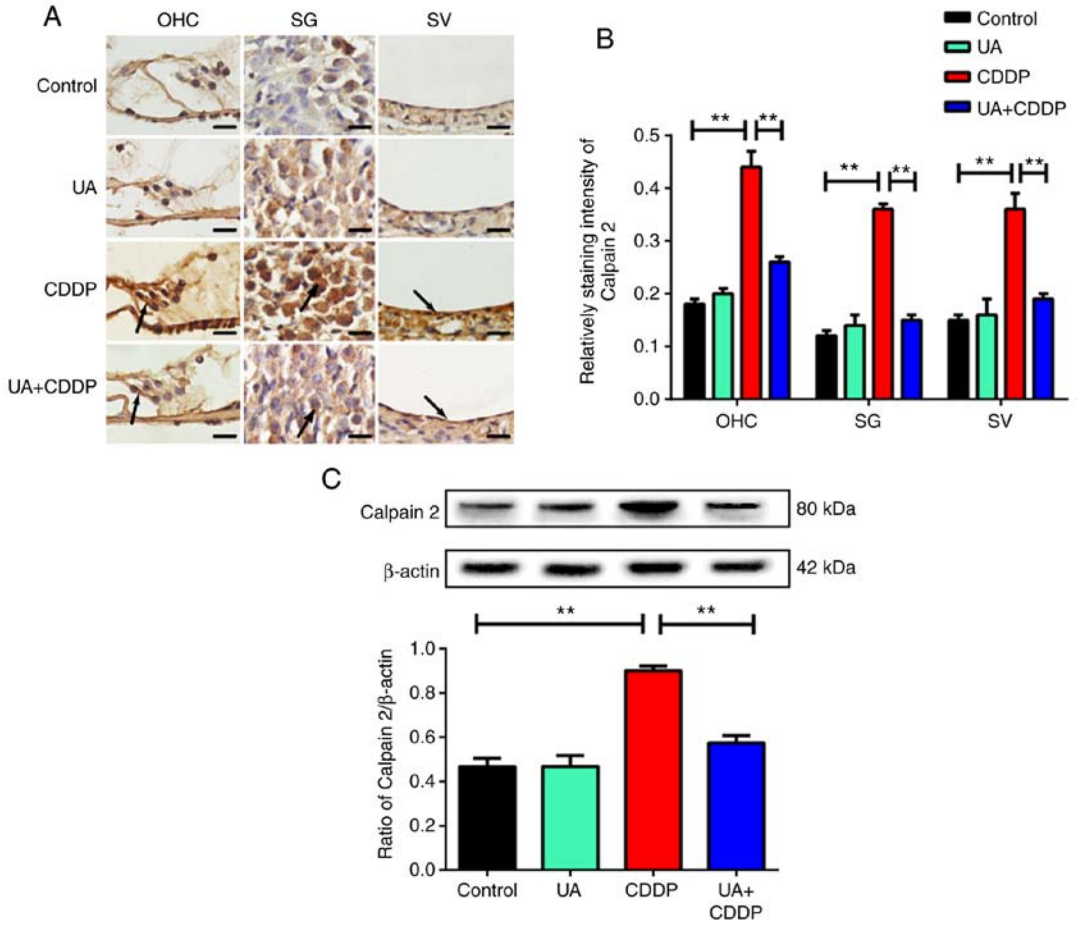

Figure 3. Effect of UA on CDDP-induced expression of calpain 2 in mouse cochlea. (A) Representative immunohistochemical staining images (brown and yellow granules) of calpain 2 on the organ of Corti, SG and SV of the cochleae. Arrows indicate the location of calpain 2-positive expression. Scale bar, 20 μm. (B) Quantification of calpain 2 immunolabeling in the different groups. n=3 ears for each group. **P<0.01. (C) Western blot analysis of calpain 2 was used to detect protein expression of calpain 2 in cochlea, with β-actin as a loading control. n=6 ears for each group. Mean values were obtained from n=3 independent experiments. **P<0.01. UA, ursolic acid; CDDP, cisplatin; SG, spiral ganglion; SV, stria vascularis.

the expression levels of these proteins significantly increased compared with the control group (P<0.01; Figs. 2B and 3B). In the UA + CDDP group, TRPV1 and calpain 2 staining was uniformly distributed, and expression significantly decreased compared with the CDDP group (P<0.01, respectively; Figs. 2B and 3B). UA treatment alone did not affect TRPV1 and calpain 2 expression in the mouse cochlea (Figs. 2A and B and 3A and B). These results were consistent with the results of western blot analysis (P<0.01; Figs. 2C and 3C).

In the control group, Ca^{2+} staining was uniformly distributed in OHCs of the basement membrane (Fig. 4A). In the CDDP group, Ca^{2+} staining was unevenly distributed (Fig. 4A), and its intensity significantly increased compared with the control group (P<0.01; Fig. 4B). In the UA + CDDP group, Ca^{2+} staining was more uniformly distributed (Fig. 4A), with significantly lower intensity compared with the CDDP group (P<0.01; Fig. 4B). The results suggested that CDDP could cause Ca^{2+} overload, and that UA could effectively inhibit Ca^{2+} influx in mice cochleae.

UA alleviates oxidative stress in mice with CDDP-induced ototoxicity. To investigate whether UA could alleviate oxidative stress, the levels of 4-HNE were analyzed. Based on immunofluorescence results, CDDP significantly enhanced production of 4-HNE in the OHCs, SG, and SV of mouse cochlea compared with the control group (P<0.01; Fig. 5A and B). However, 4-HNE production was significantly inhibited in the UA + CDDP group compared with the CDDP group (P<0.01; Fig. 5A and B). Moreover, compared with the control group, UA treatment alone did not affect 4-HNE production in the mouse cochleae (Fig. 5B). These results were confirmed by western blot analysis of 4-HNE levels (P<0.01; Fig. 5C). The results suggested that UA could prevent an increase in oxidative stress-related markers in the cochlea of mouse treated with CDDP.

The effect of UA on the antitumor effect of CDDP. Since CDDP is used as an anticancer therapeutic, it was investigated whether UA co-treatment would impair its antitumor effects. MTT assay was performed to evaluate the viability of the human ovarian cancer cell line SKVO3 in response to CDDP, UA, and UA + CDDP. While CDDP inhibited the growth of SKVO3 cells in a dose-dependent manner (Fig. 6A), growth inhibition of SKVO3 cells was significantly enhanced following UA + CDDP (4 g/ml) treatment. Moreover, UA inhibited the growth of SKOV3 cells in a dose-dependent manner (P<0.01; Fig. 6B), suggesting that UA enhanced the antitumor effect of CDDP *in vitro*.

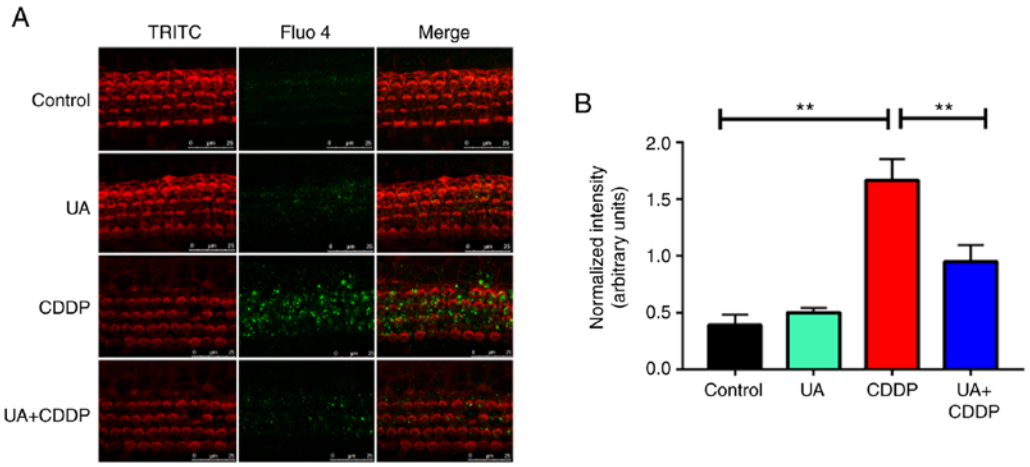

Figure 4. UA inhibits CDDP-induced calcium overload in OHCs. (A) Effect of UA on CDDP-induced measurement of Ca^{2+} levels (green) in OHCs from organotypic culture. OHCs were labeled by TRITC staining (red). Scale bar, 20 μm. (B) Quantitative levels of Fluo-4 Ca^{2+} signals from the cochlea. n=3 ears for each group. Mean values were obtained from n=3 independent experiments. **P<0.01. TRITC, tetramethylrhodamine; UA, ursolic acid; CDDP, cisplatin; OHC, outer hair cell.

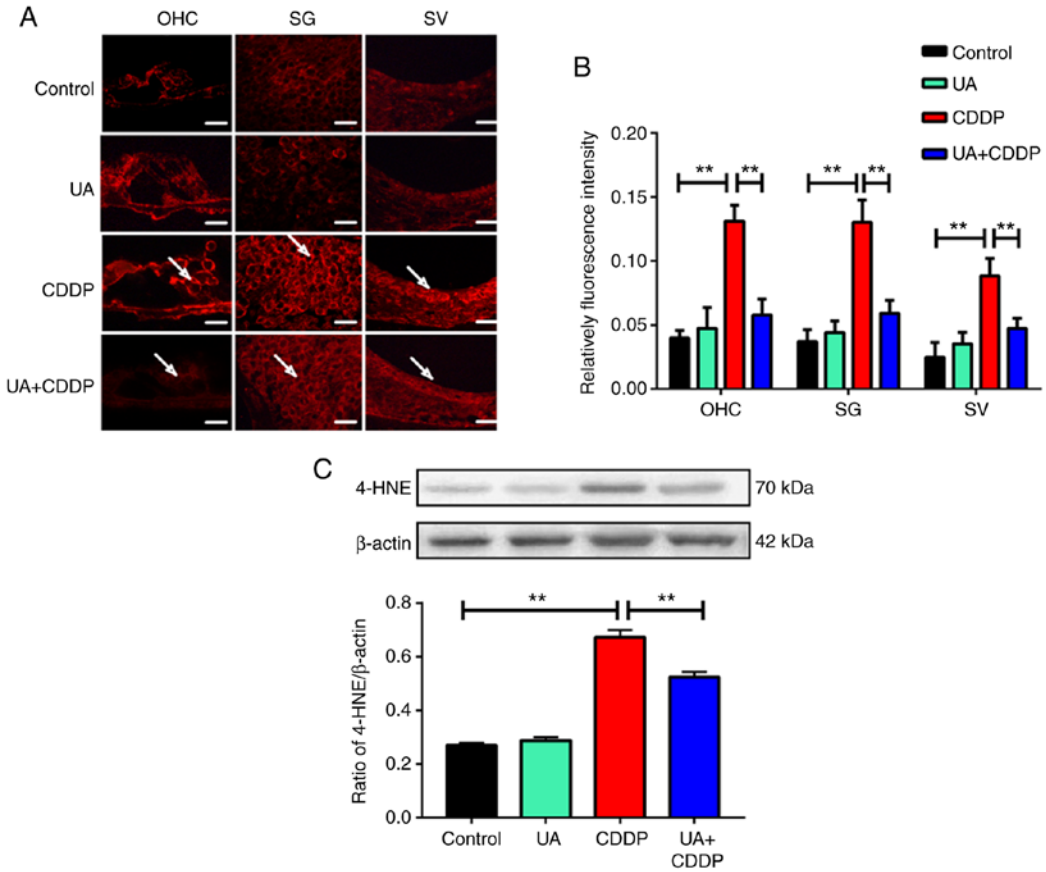

Figure 5. UA alleviates oxidative stress in the mouse cochlea with CDDP-induced ototoxicity. (A) Effect of UA on CDDP-induced expression of 4-HNE (red) in mouse cochlea. Images of paraffin sections of the organ of Corti, SG and SV were from the cochleae. Arrows indicate the location of 4-HNE-positive expression. Scale bar, 20 μm. (B) Comparison of the relative fluorescence intensity values for 4-HNE in three different sites of the mouse cochlea. n=3 ears for each group. **P<0.01. (C) Western blot analysis was used to detect protein expression of 4-HNE in the cochlea, with β-actin as a loading control. n=6 ears for each group. Mean values were obtained from n=3 independent experiments. **P<0.01. UA, ursolic acid; CDDP, cisplatin; OHC, outer hair cell; 4-HNE, 4-hydroxynonenal.

Discussion

UA is a triterpenoid compound found in >60 varieties of plants, including bearberry, Chinese elder herb and hawthorn (37). The therapeutic effects of UA include sedative, anti-inflammatory, anti-ulcer and anti-diabetic effects (38,39). A previous study demonstrated that UA significantly alleviated hydrogen peroxide-induced apoptosis against HEI-OC1

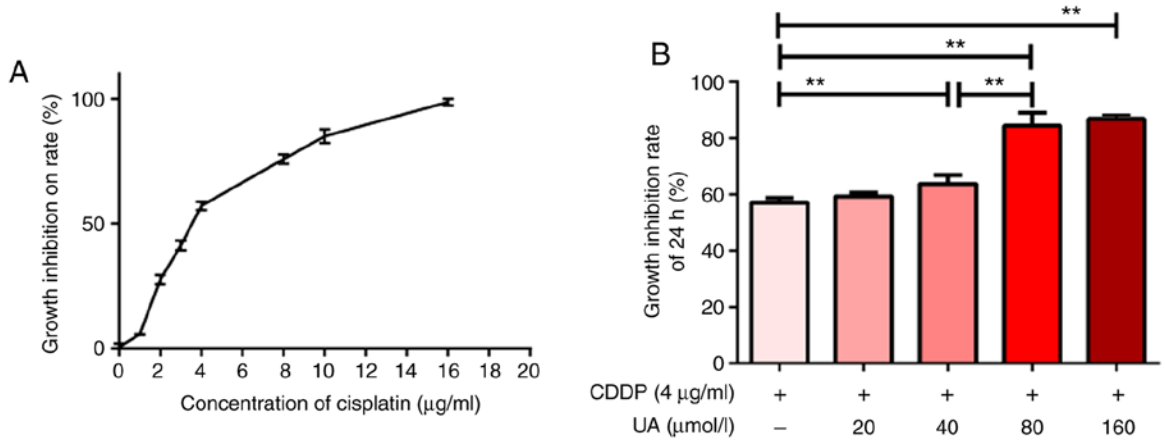

Figure 6. Effects of UA on the antitumor effect of CDDP. (A) Inhibitory effect of CDDP on the growth of SKVO3 cells. CDDP at a concentration of 4 μg/ml was determined as the optimal inhibitory concentration based on growth inhibition rate after 24 h. (B) The inhibitory effect of CDDP combined with different concentrations of UA on SKVO3 cells. n=6 for each group. Mean values were obtained from n=3 independent experiments. **P<0.01. UA, ursolic acid; CDDP, cisplatin.

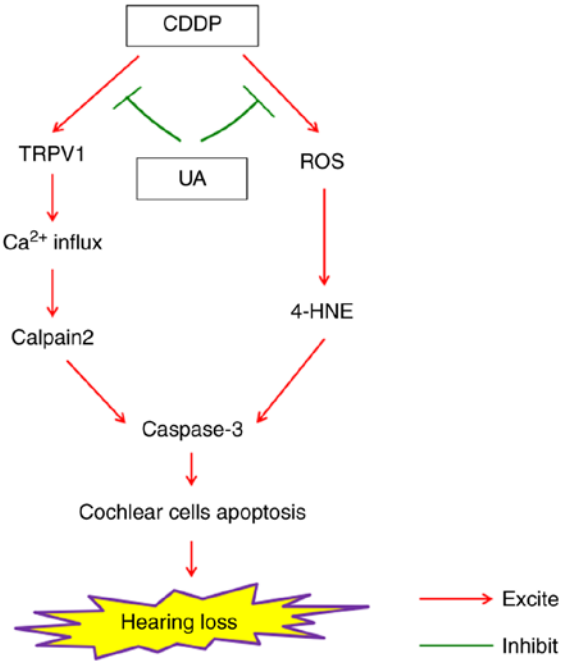

Figure 7. Possible mechanism of UA preventing CDDP-induced hearing loss in mice. CDDP, cisplatin; UA, ursolic acid; TRPV1, transient receptor potential vanilloid receptor 1; 4-HNE, 4-hydroxynonenal.

cells *in vitro* (40). In the present study, UA was found to inhibit CDDP-induced cochlear OHC damage, which in turn significantly attenuated hearing loss at low and high frequencies in mice. Therefore, based on the present findings, it was proposed that UA could provide therapeutic benefits for CDDP-induced ototoxicity.

TRPV1 channels are highly permeable to intracellular calcium influx, and overexpression of TRPV1 induces Ca^{2+} overload and the activation of calpains, especially calpain 2 (41). Activation of calpain 2 might mediate caspase-3-dependent apoptosis of cochlear cells by down-regulating Bcl-xl and up-regulating Bax (42-45). The TRPV1 channel was previously reported to play a critical role in CDDP-induced ototoxicity (46). Moreover, several studies have shown that TRPV1 expression is significantly increased in OHC, SG and SV in the cochlea in response to CDDP treatment (47-49). The present study found that UA decreased the levels of CDDP-mediated TRPV1 protein expression in the cochlear OHC, SG, and SV. In addition, CDDP dysregulated Ca^{2+} homeostasis in the cochlea, which is accompanied by increased expression of calpain 2. UA was previously shown to alleviate coughing via TRPV1 channel desensitization (50). Whether a similar mechanism can account for inhibition of CDDP-mediated TRPV1 protein expression by UA remains to be elucidated. TRPV1 is also activated by heat (>42˚C), capsaicin, low extracellular pH and oxidative stress products (51). Thus, the antioxidant activity of UA might inhibit activation of the TRPV1 channel by reducing oxidative stress products in the cochlea. The present results suggested that UA significantly blocked CDDP-induced Ca^{2+} overload in hair cells and also inhibited calpain 2 expression. These results suggested an association between the TRPV1 channel and the Ca^{2+}/calpain signaling pathway, which might explain the decrease in CDDP-induced Ca^{2+} influx observed in the cochlea following UA treatment.

Oxidative stress is considered to be an important cause of CDDP-induced hearing loss (52). The main source of ROS is NADPH oxidase (NOX) (53). CDDP induced expression of NOX3 in the cochlea, resulting in the formation of ROS, and consequently lipid peroxidation of the cochlea (10). In the present study, the levels of 4-HNE, a highly toxic lipid peroxidation product of aldehydes (54), were observed to increase as a result. High 4-HNE levels can induce the release of cytochrome *c* from the mitochondria by activating the mitogen-activated protein kinase/JNK cell death signal cascade (55). In the cytoplasm, cytochrome *c* activates caspase-9 and caspase-3, eventually leading to apoptosis of cochlear cells (56,57). Studies have shown that UA exerts significant antioxidant effects, inhibiting excessive free radical production by upregulation of endothelial nitric oxide synthase expression and downregulation of inducible nitric oxide synthase and NOX expression (58-60). In addition, UA might play an antioxidant role by enhancing free radical

scavenging (61). Consistent with these studies, the present study found that UA inhibited the production of the highly toxic lipid peroxidation product 4-HNE in the cochlea, indicating that UA could inhibit CDDP-induced lipid peroxidation.

Antioxidants such as tiopronin, resveratrol, and vitamin E can alleviate inner ear damage caused by CDDP (62-64). However, most of these antioxidants have been found to attenuate the antitumor effects of CDDP, making them a poor therapeutic option for reducing CDDP-induced ototoxicity (65). Previous research has shown that UA can exert antitumor effects by promoting cancer cell apoptosis, inhibiting tumor angiogenesis and reducing cytotoxicity, and that it might have therapeutic effects on several tumors, including gastric, liver and ovarian cancers (66-68). The present study found that UA enhanced CDDP-induced tumor cell apoptosis *in vitro*. It was hypothesized that UA may complement cisplatin in its antitumor effect. These results suggested the potential of UA and CDDP co-treatment for the treatment of solid tumors.

In conclusion, the present study found a role in the TRPV1/Ca^{2+}/calpain signaling pathway, which may facilitate CDDP-induced hearing loss. UA can reduce the extent of calcium overload and oxidative stress, and subsequently decrease the induction of apoptotic pathways associated with OHC loss (Fig. 7). These results suggested that UA can function as a lead compound for the pharmacological control of drug-induced ototoxicity.

Acknowledgements

We thank Professor Ming-Sheng Zhou from the Department of Physiology, Shenyang Medical College, China for helpful discussions and comments.

Funding

This study was supported by grants from the National Natural Science Foundation of China (grant nos. 81674036 and 81704127), the Liaoning Natural Science Foundation (grant nos. 2019-ZD-0832 and 20180550402), the Doctoral Scientific Research Foundation of Liaoning Province (grant no. 20170520045) and College Students' Innovation and Entrepreneurship Training Program (grant nos. 201710160000214, 201710160000154 and 201910160112).

Availability of data and materials

The datasets generated and/or analyzed during the current study are available from the corresponding author on reasonable request.

Authors' contributions

YD was responsible for the study design and implementation, data analysis and manuscript preparation. TX interpreted the data and wrote the manuscript. YT, TM, DQ, YW and DB were responsible for data collection and statistical analysis. YL, LY, SL and AW played an important role in study design and guidance and were responsible for the revision of the manuscript. All authors read and approved the final manuscript.

Ethics approval and consent to participate

All animal studies complied with the regulations for the Management of Laboratory Animals published by the Ministry of Science and Technology of the People's Republic of China, and all animal protocols were approved by the Animal Care and Use Committee of Jinzhou Medical University

Patient consent for publication

Not applicable.

Competing interests

The authors declare that they have no competing interests.

References

1. Basu A, Bhattacharjee A, Samanta A and Bhattacharya S: An oxovanadium(IV) complex protects murine bone marrow cells against cisplatin-induced myelotoxicity and DNA damage. Drug Chem Toxicol 40: 359-367, 2017.
2. Vera O, Jimenez J, Pernia O, Rodriguez-Antolin C, Rodriguez C, Sanchez Cabo F, Soto J, Rosas R, Lopez-Magallon S, Esteban Rodriguez I, *et al*: DNA methylation of miR-7 is a mechanism involved in platinum response through MAFG overexpression in cancer cells. Theranostics 7: 4118-4134, 2017.
3. van As JW, van den Berg H and van Dalen EC: Different infusion durations for preventing platinum-induced hearing loss in children with cancer. Cochrane Database Syst Rev 7: CD010885, 2018.
4. Klumpers MJ, Coenen MJ, Gidding CE and Te Loo DM: The role of germline variants in chemotherapy outcome in brain tumors: A systematic review of pharmacogenetic studies. Pharmacogenomics 18: 501-513, 2017.
5. Pang J, Xiong H, Zhan T, Cheng G, Jia H, Ye Y, Su Z, Chen H, Lin H, Lai L, *et al*: Sirtuin 1 and autophagy attenuate cisplatin-induced hair cell death in the mouse cochlea and zebrafish lateral line. Front Cell Neurosci 12: 515, 2019.
6. Ryu NG, Moon IJ, Chang YS, Kim BK, Chung WH, Cho YS and Hong SH: Cochlear implantation for profound hearing loss after multimodal treatment for neuroblastoma in children. Clin Exp Otorhinolaryngol 8: 329-334, 2015.
7. Youm I, West MB, Li W, Du X, Ewert DL and Kopke RD: siRNA-loaded biodegradable nanocarriers for therapeutic MAPK1 silencing against cisplatin-induced ototoxicity. Int J Pharm 528: 611-623, 2017.
8. Guo X, Bai X, Li L, Li J and Wang H: Forskolin protects against cisplatin-induced ototoxicity by inhibiting apoptosis and ROS production. Biomed Pharmacother 99: 530-536, 2018.
9. Martín-Saldaña S, Palao-Suay R, Aguilar MR, Ramírez-Camacho R and San Román J: Polymeric nanoparticles loaded with dexamethasone or α-tocopheryl succinate to prevent cisplatin-induced ototoxicity. Acta Biomater 53: 199-210, 2017.
10. Mukherjea D, Jajoo S, Sheehan K, Kaur T, Sheth S, Bunch J, Perro C, Rybak LP and Ramkumar V: NOX3 NADPH oxidase couples transient receptor potential vanilloid 1 to signal transducer and activator of transcription 1-mediated inflammation and hearing loss. Antioxid Redox Signal 14: 999-1010, 2011.
11. Kim SJ, Park C, Lee JN and Park R: Protective roles of fenofibrate against cisplatin-induced ototoxicity by the rescue of peroxisomal and mitochondrial dysfunction. Toxicol Appl Pharmacol 353: 43-54, 2018.
12. Fetoni AR, Eramo SL, Paciello F, Rolesi R, Podda MV, Troiani D and Paludetti G: Curcuma longa (curcumin) decreases in vivo cisplatin-induced ototoxicity through heme oxygenase-1 induction. Otol Neurotol 35: e169-e177, 2014.
13. Harris MS, Gilbert JL, Lormore KA, Musunuru SA and Fritsch MH: Cisplatin ototoxicity affecting cochlear implant benefit. Otol Neurotol 32: 969-972, 2011.
14. Ceriani F, Hendry A, Jeng JY, Johnson SL, Stephani F, Olt J, Holley MC, Mammano F, Engel J, Kros CJ, *et al*: Coordinated calcium signalling in cochlear sensory and non-sensory cells refines afferent innervation of outer hair cells. EMBO J 38: e99839, 2019.

15. Hegedűs L, Zámbó B, Pászty K, Padányi R, Varga K, Penniston JT and Enyedi Á: Molecular diversity of plasma membrane Ca^{2+} transporting ATPases: Their function under normal and pathological conditions. Adv Exp Med Biol 1131, 2020.
16. Wang X, Zhu Y, Long H, Pan S, Xiong H, Fang Q, Hill K, Lai R, Yuan H and Sha SH: Mitochondrial calcium transporters mediate sensitivity to noise-induced losses of hair cells and cochlear synapses. Front Mol Neurosci 11: 469, 2018.
17. Brito R, Sheth S, Mukherjea D, Rybak LP and Ramkumar V: TRPV1: A potential drug target for treating various diseases. Cells 3: 517-545, 2014.
18. Samanta A, Hughes TET and Moiseenkova-Bell VY: Transient receptor potential (TRP) channels. Subcell Biochem 87: 141-165, 2018.
19. Bai P, Liu Y, Xue S, Hamri GC, Saxena P, Ye H, Xie M and Fussenegger M: A fully human transgene switch to regulate therapeutic protein production by cooling sensation. Nat Med 25: 1266-1273, 2019.
20. Övey IS and Naziroğlu M: Homocysteine and cytosolic GSH depletion induce apoptosis and oxidative toxicity through cytosolic calcium overload in the hippocampus of aged mice: Involvement of TRPM2 and TRPV1 channels. Neuroscience 284: 225-233, 2015.
21. Kaneko Y and Szallasi A: Transient receptor potential (TRP) channels: A clinical perspective. Br J Pharmacol 171: 2474-2507, 2014.
22. Lima B, Sánchez M, Luna L, Agüero MB, Zacchino S, Filippa E, Palermo JA, Tapia A and Feresin GE: Antimicrobial and antioxidant activities of Gentianella multicaulis collected on the Andean Slopes of San Juan Province, Argentina. Z Naturforsch C J Biosci 67: 29-38, 2012.
23. Kaur T, Borse V, Sheth S, Sheehan K, Ghosh S, Tupal S, Jajoo S, Mukherjea D, Rybak LP and Ramkumar V: Adenosine A1 receptor protects against cisplatin ototoxicity by suppressing the NOX3/STAT1 inflammatory pathway in the cochlea. J Neurosci 36: 3962-3977, 2016.
24. Marwaha L, Bansal Y, Singh R, Saroj P, Bhandari R and Kuhad A: TRP channels: Potential drug target for neuropathic pain. Inflammopharmacology 24: 305-317, 2016.
25. Jabeen M, Ahmad S, Shahid K, Sadiq A and Rashid U: Ursolic acid hydrazide based organometallic complexes: Synthesis, characterization, antibacterial, antioxidant, and docking studies. Front Chem 6: 343, 2018.
26. Iqbal J, Abbasi BA, Ahmad R, Mahmood T, Kanwal S, Ali B, Khalil AT, Shah SA, Alam MM and Badshah H: Ursolic acid a promising candidate in the therapeutics of breast cancer: Current status and future implications. Biomed Pharmacother 108: 752-756, 2018.
27. Silva FS, Oliveira PJ and Duarte MF: Oleanolic, ursolic, and betulinic acids as food supplements or pharmaceutical agents for type 2 diabetes: Promise or illusion? J Agric Food Chem 64: 2991-3008, 2016.
28. Wan SZ, Liu C, Huang CK, Luo FY and Zhu X: Ursolic acid improves intestinal damage and bacterial dysbiosis in liver fibrosis mice. Front Pharmacol 10: 1321, 2019.
29. Kim GH, Kan SY, Kang H, Lee S, Ko HM, Kim JH and Lim JH: Ursolic acid suppresses cholesterol biosynthesis and exerts anti-cancer effects in hepatocellular carcinoma cells. Int J Mol Sci 20: 4767, 2019.
30. Yoon JH, Youn K, Ho CT, Karwe MV, Jeong WS and Jun M: p-Coumaric acid and ursolic acid from Corni fructus attenuated β-amyloid (25-35)-induced toxicity through regulation of the NF-κB signaling pathway in PC12 cells. J Agric Food Chem 62: 4911-4916, 2014.
31. Hong SY, Jeong WS and Jun M: Protective effects of the key compounds isolated from corni fructus against β-amyloid-induced neurotoxicity in PC12 cells. Molecules 17: 10831-10845, 2012.
32. Misra RC, Sharma S, Sandeep, Garg A, Chanotiya CS and Ghosh S: Two CYP716A subfamily cytochrome P450 monooxygenases of sweet basil play similar but nonredundant roles in ursane- and oleanane-type pentacyclic triterpene biosynthesis. New Phytol 214: 706-720, 2017.
33. DeBacker JR, Harrison RT and Bielefeld EC: Cisplatin-induced threshold shift in the CBA/CaJ, C57BL/6J, BALB/cJ mouse models of hearing loss. Hear Res 387: 107878, 2020.
34. Liu S, Xu T, Wu X, Lin Y, Bao D, Di Y, Ma T, Dang Y, Jia P, Xian J, *et al*: Pomegranate peel extract attenuates D-galactose-induced oxidative stress and hearing loss by regulating PNUTS/PP1 activity in the mouse cochlea. Neurobiol Aging 59: 30-40, 2017.
35. Matt T, Ng CL, Lang K, Sha SH, Akbergenov R, Shcherbakov D, Meyer M, Duscha S, Xie J, Dubbaka SR, *et al*: Dissociation of antibacterial activity and aminoglycoside ototoxicity in the 4-monosubstituted 2-deoxystreptamine apramycin. Proc Natl Acad Sci USA 109: 10984-10989, 2012.
36. Spinelli KJ and Gillespie PG: Monitoring intracellular calcium ion dynamics in hair cell populations with Fluo-4 AM. PLoS One 7: e51874, 2012.
37. Woźniak Ł, Skąpska S and Marszałek K: Ursolic acid-a pentacyclic triterpenoid with a wide spectrum of pharmacological activities. Molecules 20: 20614-20641, 2015.
38. Jinhua W: Ursolic acid: Pharmacokinetics process in vitro and in vivo, a mini review. Arch Pharm (Weinheim) 352: e1800222, 2019.
39. Xu HL, Wang XT, Cheng Y, Zhao JG, Zhou YJ, Yang JJ and Qi MY: Ursolic acid improves diabetic nephropathy via suppression of oxidative stress and inflammation in streptozotocin-induced rats. Biomed Pharmacother 105: 915-921, 2018.
40. Yu HH, Hur JM, Seo SJ, Moon HD, Kim HJ, Park RK and You YO: Protective effect of ursolic acid from Cornus officinalis on the hydrogen peroxide-induced damage of HEI-OC1 auditory cells. Am J Chin Med 37: 735-746, 2009.
41. Bao D, Zhao W, Dai C, Wan H and Cao Y: H89 dihydrochloride hydrate and calphostin C lower the body temperature through TRPV1. Mol Med Rep 17: 1599-1608, 2018.
42. Huang KF, Ma KH, Chang YJ, Lo LC, Jhap TY, Su YH, Liu PS and Chueh SH: Baicalein inhibits matrix metalloproteinase 1 expression via activation of TRPV1-Ca-ERK pathway in ultraviolet B-irradiated human dermal fibroblasts. Exp Dermatol 28: 568-575, 2019.
43. Berekméri E, Deák O, Téglás T, Sághy É, Horváth T, Aller M, Fekete Á, Köles L and Zelles T: Targeted single-cell electroporation loading of Ca indicators in the mature hemicochlea preparation. Hear Res 371: 75-86, 2019.
44. Chang L and Wang A: Calpain mediated cisplatin-induced ototoxicity in mice. Neural Regen Res 8: 1995-2002, 2013.
45. Yu L, Tang H, Jiang XH, Tsang LL, Chung YW and Chan HC: Involvement of calpain-I and microRNA34 in kanamycin-induced apoptosis of inner ear cells. Cell Biol Int 34: 1219-1225, 2010.
46. Bhatta P, Dhukhwa A, Sheehan K, Al Aameri RFH, Borse V, Ghosh S, Sheth S, Mamillapalli C, Rybak L, Ramkumar V and Mukherjea D: Capsaicin protects against cisplatin ototoxicity by changing the STAT3/STAT1 ratio and activating cannabinoid (CB2) receptors in the cochlea. Sci Rep 9: 4131, 2019.
47. Mukherjea D, Jajoo S, Whitworth C, Bunch JR, Turner JG, Rybak LP and Ramkumar V: Short interfering RNA against transient receptor potential vanilloid 1 attenuates cisplatin-induced hearing loss in the rat. J Neurosci 28: 13056-13065, 2008.
48. Rybak LP, Mukherjea D, Jajoo S, Kaur T and Ramkumar V: siRNA-mediated knock-down of NOX3: Therapy for hearing loss? Cell Mol Life Sci 69: 2429-2434, 2012.
49. Sheth S, Mukherjea D, Rybak LP and Ramkumar V: Mechanisms of cisplatin-induced ototoxicity and otoprotection. Front Cell Neurosci 11: 338, 2017.
50. Zhang Y, Sreekrishna K, Lin Y, Huang L, Eickhoff D, Degenhardt C and Xu T: Modulation of transient receptor potential (TRP) channels by chinese herbal extracts. Phytother Res 25: 1666-1670, 2011.
51. Wang S, Wang S, Asgar J, Joseph J, Ro JY, Wei F, Campbell JN and Chung MK: Ca^{2+} and calpain mediate capsaicin-induced ablation of axonal terminals expressing transient receptor potential vanilloid 1. J Biol Chem 292: 8291-8303, 2017.
52. González-García JA, Nevado J, García-Berrocal JR, Sánchez-Rodríguez C, Trinidad A, Sanz R and Ramírez-Camacho R: Endogenous protection against oxidative stress caused by cisplatin: Role of superoxide dismutase. Acta Otolaryngol 130: 453-457, 2010.
53. Peng X, Yang Y, Tang L, Wan J, Dai J, Li L, Huang J, Shen Y, Lin L, Gong X and Zhang L: Therapeutic benefits of apocynin in mice with lipopolysaccharide/D-galactosamine-induced acute liver injury via suppression of the late stage pro-apoptotic AMPK/JNK pathway. Biomed Pharmacother 125: 110020, 2020.
54. Zhang Y, Xu K, Kerwin T, LaManna JC and Puchowicz M: Impact of aging on metabolic changes in the Ketotic rat brain: Glucose, oxidative and 4-HNE metabolism. Adv Exp Med Biol 1072: 21-25, 2018.
55. Wang L, He T, Wan B, Wang X and Zhang L: Orexin A ameliorates HBV X protein-induced cytotoxicity and inflammatory response in human hepatocytes. Artif Cells Nanomed Biotechnol 47: 2003-2009, 2019.

56. Hsu CL, Hong BH, Yu YS and Yen GC: Antioxidant and anti-inflammatory effects of Orthosiphon aristatus and its bioactive compounds. J Agric Food Chem 58: 2150-2156, 2010.
57. Yang EJ, Moon JY, Lee JS, Koh J, Lee NH and Hyun CG: Acanthopanax koreanum fruit waste inhibits lipopolysaccharide-induced production of nitric oxide and prostaglandin E2 in RAW 264.7 macrophages. J Biomed Biotechnol 2010: 715739, 2010.
58. Mu H, Liu H, Zhang J, Huang J, Zhu C, Lu Y, Shi Y and Wang Y: Ursolic acid prevents doxorubicin-induced cardiac toxicity in mice through eNOS activation and inhibition of eNOS uncoupling. J Cell Mol Med 23: 2174-2183, 2019.
59. Zhang C, Wang C, Li W, Wu R, Guo Y, Cheng D, Yang Y, Androulakis IP and Kong AN: Pharmacokinetics and pharmacodynamics of the triterpenoid ursolic acid in regulating the antioxidant, anti-inflammatory, and epigenetic gene responses in rat leukocytes. Mol Pharm 14: 3709-3717, 2017.
60. Yu SS, Chen B, Huang CK, Zhou JJ, Huang X, Wang AJ, Li BM, He WH and Zhu X: Ursolic acid suppresses TGF-β1-induced quiescent HSC activation and transformation by inhibiting NADPH oxidase expression and Hedgehog signaling. Exp Ther Med 14: 3577-3582, 2017.
61. Antônio E, Antunes ODR Junior, de Araújo IS, Khalil NM and Mainardes RM: Poly(lactic acid) nanoparticles loaded with ursolic acid: Characterization and in vitro evaluation of radical scavenging activity and cytotoxicity. Mater Sci Eng C Mater Biol Appl 71: 156-166, 2017.
62. Fetoni AR, Sergi B, Ferraresi A, Paludetti G and Troiani D: Protective effects of alpha-tocopherol and tiopronin against cisplatin-induced ototoxicity. Acta Otolaryngol 124: 421-426, 2004.
63. Chirtes F and Albu S: Prevention and restoration of hearing loss associated with the use of cisplatin. Biomed Res Int 2014: 925485, 2014.
64. Luo J, Hu YL and Wang H: Ursolic acid inhibits breast cancer growth by inhibiting proliferation, inducing autophagy and apoptosis, and suppressing inflammatory responses via the PI3K/AKT and NF-κB signaling pathways *in vitro*. Exp Ther Med 14: 3623-3631, 2017.
65. Chang HY, Chen CJ, Ma WC, Cheng WK, Lin YN, Lee YR, Chen JJ and Lim YP: Modulation of pregnane X receptor (PXR) and constitutive androstane receptor (CAR) activation by ursolic acid (UA) attenuates rifampin-isoniazid cytotoxicity. Phytomedicine 36: 37-49, 2017.
66. Kim SH, Jin H, Meng RY, Kim DY, Liu YC, Chai OH, Park BH and Kim SM: Activating hippo pathway via Rassf1 by ursolic acid suppresses the tumorigenesis of gastric cancer. Int J Mol Sci 20: 4709, 2019.
67. Wang WJ, Sui H, Qi C, Li Q, Zhang J, Wu SF, Mei MZ, Lu YY, Wan YT, Chang H and Guo PT: Ursolic acid inhibits proliferation and reverses drug resistance of ovarian cancer stem cells by downregulating ABCG2 through suppressing the expression of hypoxia-inducible factor-1α in vitro. Oncol Rep 36: 428-440, 2016.
68. Zhou M, Yi Y, Liu L, Lin Y, Li J, Ruan J and Zhong Z: Polymeric micelles loading with ursolic acid enhancing anti-tumor effect on hepatocellular carcinoma. J Cancer 10: 5820-5831, 2019.